Electron-Phonon Interaction at the Be(0001) Surface

A. Eiguren,[1] S. de Gironcoli,[2] E.V. Chulkov,[1,3] P.M. Echenique,[1,3] and E. Tosatti[2,4]

[1]*Departmento de Física de Materiales and Centro Mixto CSIC-UPV/EHU, Facultad de Ciencias Químicas, Universidad del Pais Vasco/Euskal Herriko Unibertsitatea, Adpo. 1072, 20018 San Sebastián/Donostia, Basque Country, Spain*

[2]*International School for Advanced Studies (SISSA) and Istituto Nazionale di Fisica della Materia (INFM/DEMOCRITOS), via Beirut 2-4, I-34014, Trieste, Italy*

[3]*Donostia International Physics Center (DIPC), Paseo de Manuel Lardizabal, 4, 20018 San Sebastián/Donostia, Spain*

[4]*International Centre for Theoretical Physics (ICTP), P.O. Box 586, I-34014, Trieste, Italy*

(Received 30 May 2003; published 17 October 2003)

We present a first principle study of the electron-phonon (e-p) interaction at the Be(0001) surface. The real and imaginary parts of the e-p self-energy (Σ) are calculated for the $\bar{\Gamma}$ surface state in the binding energy range from the $\bar{\Gamma}$ point to the Fermi level. Our calculation shows an overall good agreement with several photoemission data measured at high and low temperatures. Additionally, we show that the energy derivative of ReΣ presents a strong temperature and energy variation close to E_F, making it difficult to measure its value just at E_F.

DOI: 10.1103/PhysRevLett.91.166803 PACS numbers: 73.20.–r, 68.35.Ja, 71.10.–w, 74.78.–w

For many years now a considerable effort has been directed toward the study of electron-phonon (e-p) effects and quasiparticle dynamics in low dimensional systems. Important examples include semiconductor heterostructures, superconducting materials with layered structures, and electrons in two-dimensional surface states. Experimentally, e-p effects are becoming increasingly accessible on surfaces, through powerful techniques like high resolution angular-resolved photoemission spectroscopy, scanning tunnelling spectroscopy, and time-resolved two-photon photoemission spectroscopy.

Be(0001) offers in this respect a textbook study case. Here the surface states form a fully metallic, high density two-dimensional electron gas, rather well decoupled from the bulk Be substrate, itself only of semimetal character [1,2]. The surface states increase the density of electron states (DOS) at the Fermi energy (E_F) by a factor of 4–5 in the surface layer [2]. This radical change of character between surface and bulk goes along with some other very special properties of the Be(0001) surface [3]. Following the DOS arguments, the surface λ parameter, representative of the e-p interaction, is believed to be about a factor of 4–5 larger than in bulk Be [4–7]. Values of λ ranging from 0.65 to 1.2 were obtained from the high temperature surface state broadening [4], or by fitting the real part of the low temperatures surface state self-energy to simple models [5–7]. The scatter between these values is disturbing. Also, a value as large as 1.2 may raise questions concerning the stability of the normal metallic state of this surface. On the other hand, it is well known that simple model calculations, such as Debye models, are surely too crude, neglecting band structure effects and the important contribution of the surface phonon modes [8]. Electron energy-loss spectroscopy measurements [9] showed that the surface phonon dispersions at Be(0001) do qualitatively differ from those obtained by using truncated bulk models [9].

In this Letter we present the first parameter-free *ab initio* calculation of the e-p interaction at a real metal surface, Be(0001), that contains all the ingredients entering the e-p interaction, namely, surface electron and phonon states, as well as electronic screening. Our detailed analysis results in excellent agreement with all experimental data. We also motivate more future experimental work.

A fully relaxed 12 layer slab has been considered. We have used the density-functional theory in the local density approximation (LDA). The e-p matrix elements and phonon frequencies were calculated using density-functional perturbation theory [10], through the PWSCF program [11]. A norm conserving pseudopotential was used with a cutoff of 22 Ry for the expansion of the electronic wave function in plane waves. For the Brillouin zone electronic structure integrations an order one Hermite-Gauss smearing technique was used, with smearing parameter $\sigma = 0.05$ Ry and as many as 102 special $\mathbf{k}$ points in the irreducible wedge of the 2D Brillouin zone (IWBZ). The linear response calculation for phonon modes [10] has been performed with 30 special q points in the IWBZ, yielding surface phonons in excellent agreement with experiments [9] and previous calculations [12].

The basic quantity in the study of the e-p interaction is the so-called Eliashberg function (ELF) [13]. This function measures the phonon density of states weighted by the e-p interaction. It represents the probability of emitting a phonon of energy ω at $T = 0$

$$\alpha^2 F_i(\omega, E) = \int \frac{d^2\vec{k}}{\Omega_{\mathrm{BZ}}} \frac{\delta(E - E_{i,\vec{k}})}{N_i(E)} \times \int \frac{d^2\vec{q}}{\Omega_{\mathrm{BZ}}} \sum_{\nu}^{f} |g^{i,f,\nu}_{\vec{k},\vec{k}+\vec{q}}|^2 \delta(E - E_{f,\vec{k}+\vec{q}}) \delta(\omega - \omega^{\nu}_{\vec{q}}). \quad (1)$$

The ELF contains all the information needed for the calculation of the real and imaginary parts of the self-energy. In Eq. (1), $g^{i,f,\nu}_{\vec{k},\vec{k}+\vec{q}} = \langle \Psi_{i,\vec{k}} | \Delta_{\mathrm{SCF}} V^{\nu}_{\vec{q}} | \Psi_{f,\vec{k}+\vec{q}} \rangle$ is the e-p matrix element where Ψ are the electronic state wave functions and $\Delta_{\mathrm{SCF}} V^{\nu}_{\vec{q}}$ denotes the change of the self-consistent electron potential induced by a phonon mode with momentum $\vec{q}$ and mode index ν; i refers to the electronic state (surface state) index, f to the final state, E denotes the binding energy, $N_i(E)$ the i state partial density of states at energy E, and Ω_{BZ} is the area of the 2D Brillouin zone.

The imaginary part of the self-energy related to the lifetime of the excited electronic state through $\tau^{-1} = 2\mathrm{Im}\Sigma$ can be written in terms of the ELF,

$$\mathrm{Im}\Sigma^0_i(E;T) = \pi \int_0^\infty d\omega \alpha^2 F_i(\omega, E)[1 - f(E-\omega) + f(E+\omega) + 2n(\omega)], \quad (2)$$

where f and n are the Fermi and Bose distribution functions, respectively. The real part reflects renormalization of the electronic band due to the interaction with phonons and can also be calculated from the ELF [13],

$$\mathrm{Re}\Sigma_i(E;T) = \int_{-\infty}^{\infty} d\nu \int_0^\infty d\omega \alpha^2 F_i(\omega, E) \frac{2\omega}{\nu^2 - \omega^2} f(\nu + E). \quad (3)$$

For the calculation of the ELF, the **k** integration was carried out with 102 special points in the IWBZ and with 30 points for the **q** integration. The two Dirac deltas containing the electron band energies were again replaced by order one Hermite-Gauss smearing functions. In order to gain confidence in the convergence of the calculation, we performed a set of calculations with different smearing parameters in the range 0.0025–0.1 Ry, which gives an estimated error of ~5% for the surface state broadening at all energies except inside a window of 0.4 eV around E_F where we estimate an error of ~15%.

Figure 1 shows the electron and phonon band structures. In the upper panel of Fig. 1 the $\bar{\Gamma}$ point surface state band sticks out (green line); near the $\bar{M}$ point another surface electronic state also appears. In the lower panel, the phonon dispersions are shown. The Rayleigh wave (red line) is a surface localized phonon mode polarized mainly along the surface normal. This and other surface phonon modes are visible within the surface band gaps.

Figure 2 shows the calculated ELF for a hole at E_F (upper panel) and at the $\bar{\Gamma}$ point (lower panel). The ELF is broken up into contributions corresponding to the intraband scattering (green line) and the Rayleigh mode scattering contribution (red line). From the upper panel of Fig. 2, the decay of the hole at E_F is dominated by the intraband scattering contribution (green line). The sum of the contributions from the decay into the $\bar{M}$ point surface state (not represented) and the intraband contribution (green line) gives ~90% of the total (solid line) at E_F.

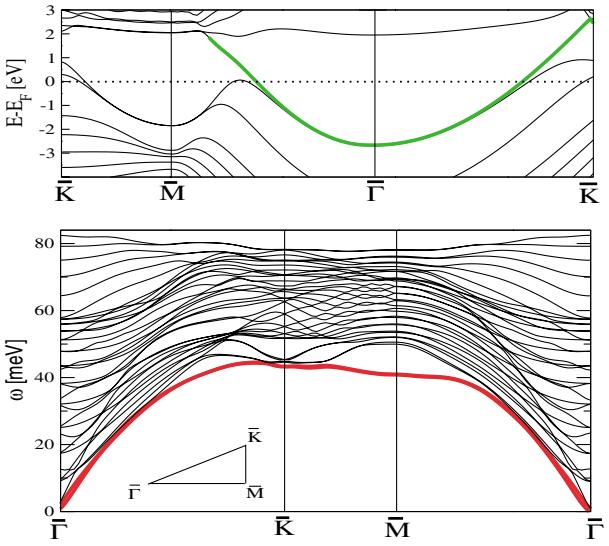

FIG. 1 (color). Top panel shows the electronic band structure of a fully relaxed 12 layer Be(0001) slab; the $\bar{\Gamma}$ surface state is indicated by the green line. Bottom panel shows the phonon dispersions, where the red line represents the Rayleigh mode.

Thus, the decay process of the hole at E_F is sharply confined in space to almost exclusively the surface state region. By contrast, the character of the interaction changes radically for the hole at the $\bar{\Gamma}$ point (lower panel), for which the decay into bulk states dominates.

Photoemission experiments enable the measurement of the high temperature behavior of the broadening, $\Gamma(E) = 2\pi k_B T \lambda_0(E)$, for a state with arbitrary binding energy E [4,8]. Theoretically $\lambda_0(E)$ is determined by the first reciprocal moment of the ELF [13].

$$\lambda_0(E) \equiv 2 \int_0^\infty d\omega \frac{\alpha^2 F(\omega, E)}{\omega}. \quad (4)$$

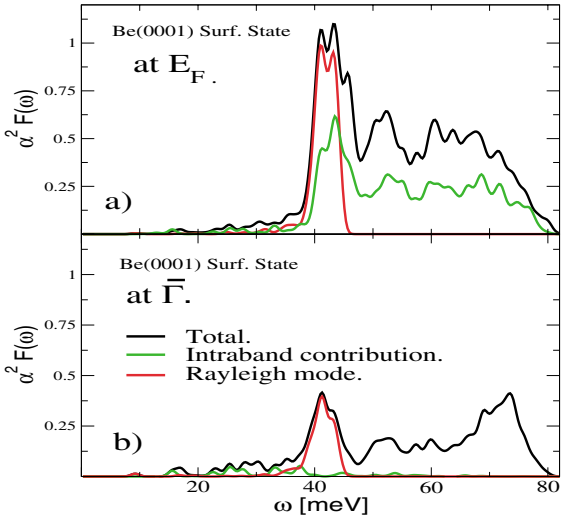

FIG. 2 (color). Different contributions to the Eliashberg function for the hole state (a) at E_F, (b) at $\bar{\Gamma}$ point.

Equation (4) indicates an enhanced role of the ELF at low energies. Figure 2 shows that the weight of the surface phonon modes is concentrated around $\omega_D/2$ ($\omega_D \simeq 80$ meV), thus a fitting procedure of the λ_0 parameter through a Debye model [$\alpha^2F = \lambda_0(\omega/\omega_D)^2$] will give rise in this case to an excessive low temperature broadening compared to a more realistic calculation using the same Debye energy ω_D and λ_0. The top panel of Fig. 3 shows the real (orange line) and imaginary part (black line) of the self-energy calculated for $T = 0$ and as a function of the binding energy. The imaginary part is resolved into contributions coming from intraband scattering (green line) and the contribution of the Rayleigh mode (red line). The imaginary part varies by a factor of 2 going from E_F to the $\bar{\Gamma}$ point. The bottom panel of Fig. 3 shows the variation of the λ_0 parameter defined through Eq. (4) as a function of the binding energy. From this figure we deduce that the temperature derivative of the high-T surface state broadening is twice that of the hole at the E_F compared to that at the $\bar{\Gamma}$ point.

Recently, the identity between the partial derivative of ReΣ at the Fermi level and $\lambda_0(E_F)$, that is $\lambda \equiv \lambda_0(E_F) = \Lambda(E_F, T = 0)$,

$$\Lambda(E, T) \equiv -\frac{\partial \mathrm{Re}\Sigma(E, T)}{\partial E} \tag{5}$$

has been used to determine the e-p coupling parameter λ [5–7]. However, it is of crucial importance here to distinguish Λ and λ_0. The results of Fig. 3 do not take into account the renormalization of electron bands due to the real part of the self-energy. We denote by E_k^0 the pure LDA unrenormalized bands and by E_k the renormalized ones

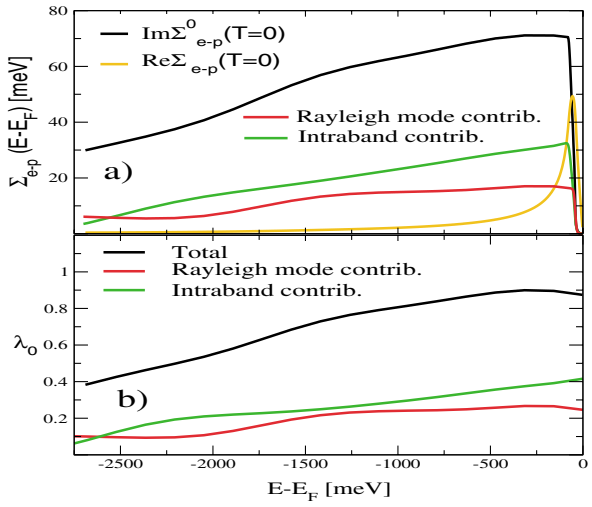

FIG. 3 (color). (a) The e-p contribution to ReΣ (orange line) and ImΣ^0 (black line) at $T = 0$ as a function of the binding energy. ImΣ^0 is broken up into contributions from the intraband scattering (green line) and contributions from the Rayleigh mode (red line). (b) The black line represents the total value of λ_0 [Eq. (4)] and the green and red lines the contributions from intraband scattering and Rayleigh mode, respectively.

including ReΣ, obtained by solving numerically the equation $E_k = E_k^0 + \mathrm{Re}\Sigma(E_k)$ [13] (see Fig. 4). It is well known that close to E_F the electron velocity, the e-p coupling form factor, and the lifetime itself are renormalized [13].

Provided that the system is isotropic and $|\Lambda(E, T)| \ll 1$, an estimation of the renormalized imaginary part [13] can be obtained from

$$\mathrm{Im}\Sigma(E_k) \simeq \frac{\mathrm{Im}\Sigma^0(E_k)}{1 + \Lambda(E_k)}, \tag{6}$$

where ImΣ denotes the renormalized quantity. While the breakdown of the approximation expressed by Eq. (6) is clear for values of $\Lambda(E, T)$ close to -1, this form generally helps us to understand how the deformation of the electronic band caused by the real self-energy affects itself the lifetime of the surface state.

In the top panel of Fig. 4, we show the unrenormalized imaginary part of the self-energy (ImΣ^0, dotted line) calculated from Eq. (2) and the renormalized ones at $T = 40$ (orange line) and at $T = 12$ K (violet line). The result for 12 K is displayed only for reasonable values of $1/(1 + \Lambda)$. These two temperatures, 12 and 40 K, are the same as those considered experimentally, Refs. [5,6], respectively. In the bottom panel, the real parts of the self-energy at $T = 12$ K (violet line) and at $T = 40$ K (orange line) are depicted. The inset of the bottom panel shows the

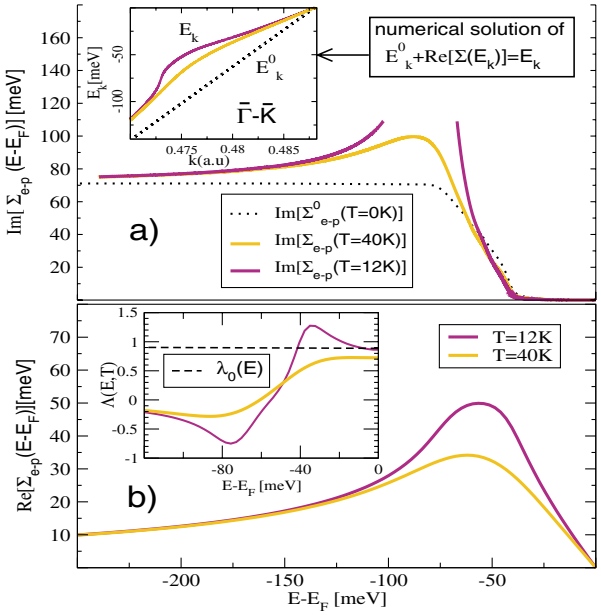

FIG. 4 (color). (a) Surface state imaginary part of the self-energy near E_F. ImΣ^0 corresponds to the unrenormalized result (Fig. 3), the renormalized ImΣ is represented for temperatures 12 (violet line) and 40 K (orange line). The inset shows modified dispersions at 12 and 40 K. (b) ReΣ near E_F at 12 and 40 K (orange line). The inset shows the quantity $\Lambda(E, T) \equiv -[\partial\Sigma(E, T)/\partial E]$. Note that at low temperature (12 K) $\Lambda(E_F, T) \simeq 0.9$ is consistent with $\lambda_0(E_F) \simeq 0.9$ from Fig. 3.

derivatives of the real part of the self-energy at these two temperatures.

In Ref. [5] a detailed measurement of ImΣ and ReΣ is reported for $T = 40$ K. An "unusual" peak of ImΣ for the hole at binding energies around the maximum phonon energy ($\sim\omega_D$) was observed. This behavior is very well described by our calculation at the same temperature (orange line). The calculated real part of the self-energy also shows excellent agreement with the measurement, and our $\Lambda(E_F, T = 40\ \mathrm{K}) \simeq 0.7$ is in excellent agreement with their measured 0.7 ± 0.1 (inset of the bottom panel of Fig. 4). In Refs. [6,7] the derivative of the real self-energy part was presented for $T = 12$ K suggesting a value of $\Lambda(E_F, T = 12\ \mathrm{K}) \simeq 1.15$. As explained in Ref. [5], this value was slightly overestimated due to the fixed angle photoemission experiment, and a corrected value of 0.87 was suggested instead. Our calculated $\Lambda(E_F, T = 12\ \mathrm{K}) \simeq 0.9$ is in excellent agreement with this corrected value (inset of bottom panel of Fig. 4). Reference [4] reported high temperature measurements of the broadening for the surface state hole at binding energy $\sim$350 meV, obtaining an estimate λ_0 ($E = 350$ meV) of 1.15 ± 0.1, which compares reasonably well with a calculated λ_0 ($E = 350$ meV) $\simeq 0.9$ (see bottom panel of Fig. 3).

Analyzing the temperature dependence of the broadening in more detail, we note that for larger T, the maximum value of the T derivative of ReΣ decreases, and so does the effect of the renormalizing denominator in Eq. (6) (Fig. 4). By contrast, increasing temperature favors phonon occupation: thus we have two competing tendencies and a minimum can be expected in the temperature dependence of ImΣ. Detailed calculation of ImΣ predicts a minimum of ImΣ around $T \sim 150$ K for states close to ω_D binding energy (see Fig. 5). It would be interesting to verify this minimum in the temperature dependence of the broadening. This effect should be even more pronounced for binding energies close to $\sim\omega_D$ where the effect of the renormalization is stronger. Here in fact the group velocity selectively rises above its bare value, and so does the low temperature hole decay rate, giving rise to a local maximum as a function of hole energy. Removal of this effect by temperature causes the local minimum predicted in Fig. 5.

In summary we presented the first parameter-free *ab initio* calculation of the *e-p* interaction in a surface state on a real metal surface, Be(0001). The surface state renormalization and its broadening were calculated, and the latter was found to agree well with existing experimental data. The energy derivative of ReΣ presents a strong energy and temperature dependence near E_F, so that an accurate measurement of $\lambda \equiv \Lambda(E_F) = \lambda_0(E_F)$ requires temperatures $T \lesssim 12$ K and energies very close to E_F. Measurements done under different conditions can produce very different λ values which explains the variety of values in literature. Additionally, the effect of the renormalization of the surface state band on its own broadening is pointed out and new experiments are suggested to confirm a new minimum predicted in the temperature dependence. Other conceivable consequences of a medium size surface state *e-p* coupling, including the possible stabilization of a 2D BCS state at $T = 0$ [14] and/or the factors hindering it, remain to be explored.

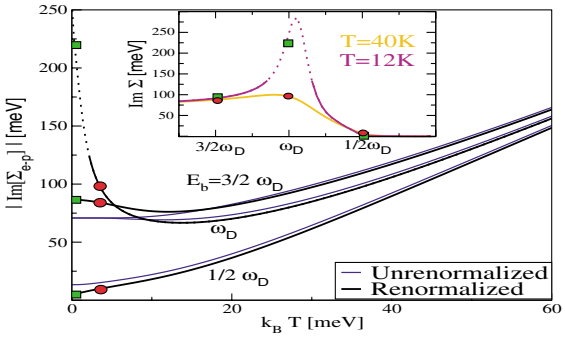

FIG. 5 (color). Temperature dependence of the broadening at $\omega_D/2$, at ω_D and at $3/2\omega_D$ binding energies. Black lines represent the renormalized broadening according to Eq. (6). Note the minimum at temperatures $k_B T \sim 13$ meV. The black dotted line for ω_D indicates the region where Eq. (6) is not reliable. The inset shows the ImΣ dependence on binding energy (E_b).

We acknowledge financial support from the Basque Government, the Max Planck Research Award Funds, the Spanish Ministerio de Educación y Ciencia (MEC), and the Basque Country University. Work in SISSA was supported through MIUR COFIN and FIRB projects, by INFM/F, and by the "Iniziativa Trasversale Calcolo Parallelo" of INFM.

[1] R. A. Bartynski *et al.*, Phys. Rev. B **32**, 1921 (1985).
[2] E. V. Chulkov *et al.*, Surf. Sci. **188**, 287 (1987).
[3] E. W. Plummer and J. B. Hannon, Prog. Surf. Sci. **46**, 149 (1994); L. I. Johansson *et al.*, Phys. Rev. Lett. **71**, 2453 (1993); P. T. Sprunger *et al.*, Science **275**, 1764 (1997).
[4] T. Balasubramanian *et al.*, Phys. Rev. B **57**, R6866 (1998).
[5] S. LaShell *et al.*, Phys. Rev. B **61**, 2371 (2000).
[6] M. Hengsberger *et al.*, Phys. Rev. Lett. **83**, 592 (1999).
[7] M. Hengsberger *et al.*, Phys. Rev. B **60**, 10 796 (1999).
[8] A. Eiguren *et al.*, Phys. Rev. Lett. **88**, 066805 (2002).
[9] J. B. Hannon *et al.*, Phys. Rev. B **53**, 2090 (1996).
[10] S. Baroni *et al.*, Rev. Mod. Phys. **73**, 515 (2001).
[11] S. Baroni *et al.*, http://www.pwscf.org
[12] M. Lazzeri *et al.*, Surf. Sci. **402**, 715 (1998).
[13] G. Grimvall, in *The Electron-Phonon Interaction in Metals*, edited by E. Wohlfarth, Selected Topics in Solid State Physics (North-Holland, New York, 1981).
[14] E. Tosatti, in *Electronic Surface and Interface States on Metallic Systems*, edited by E. Bertel and M. Donath (World Scientific, Singapore, 1995), p. 67.